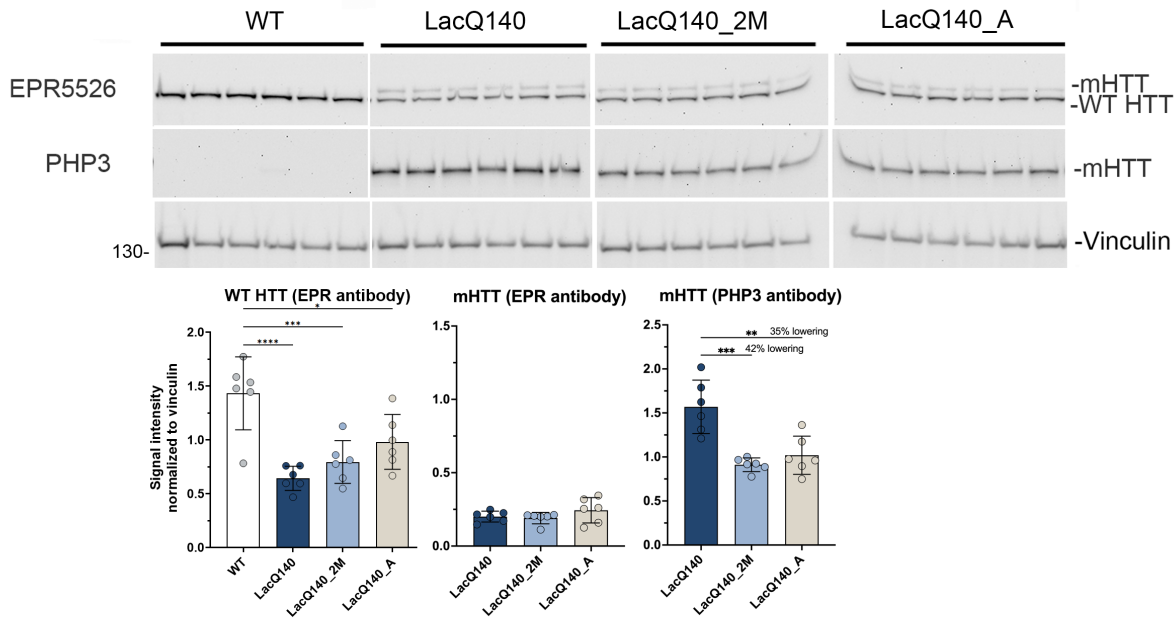
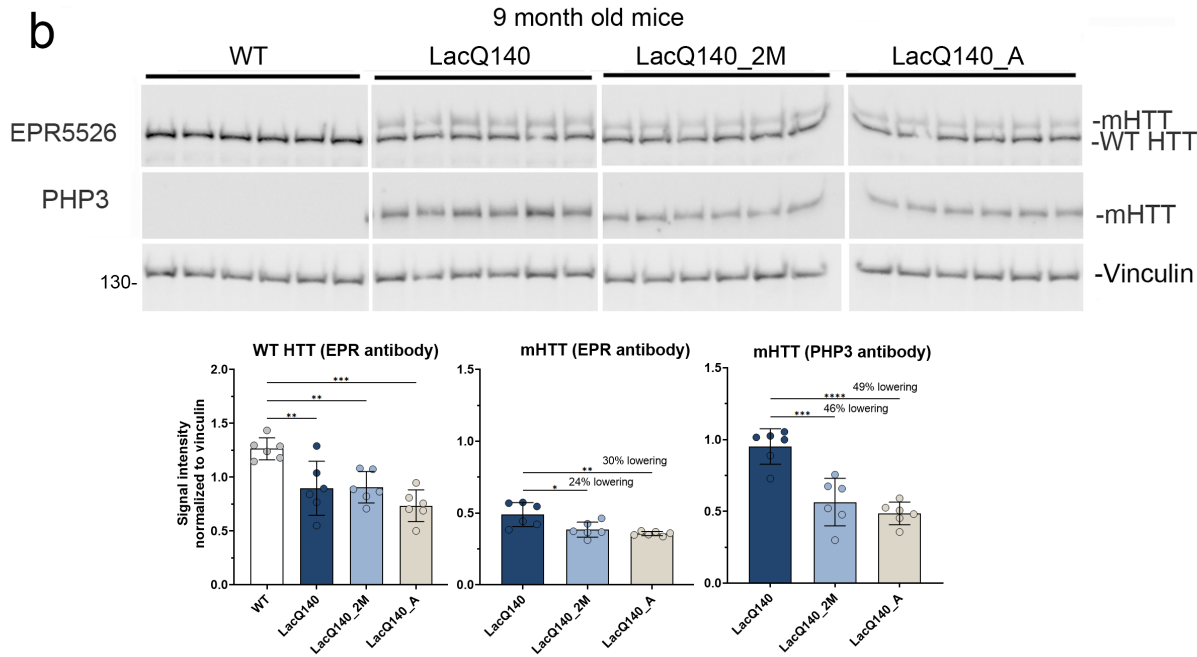


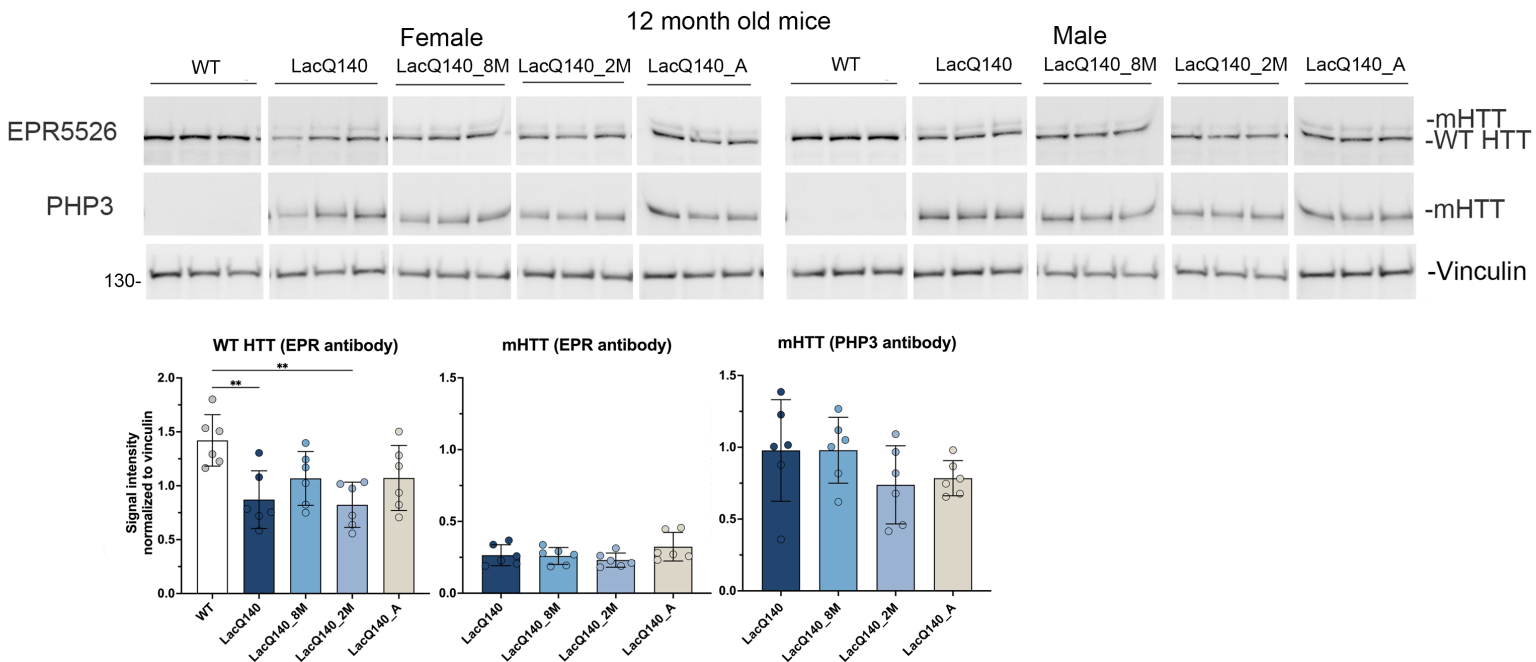
a



b



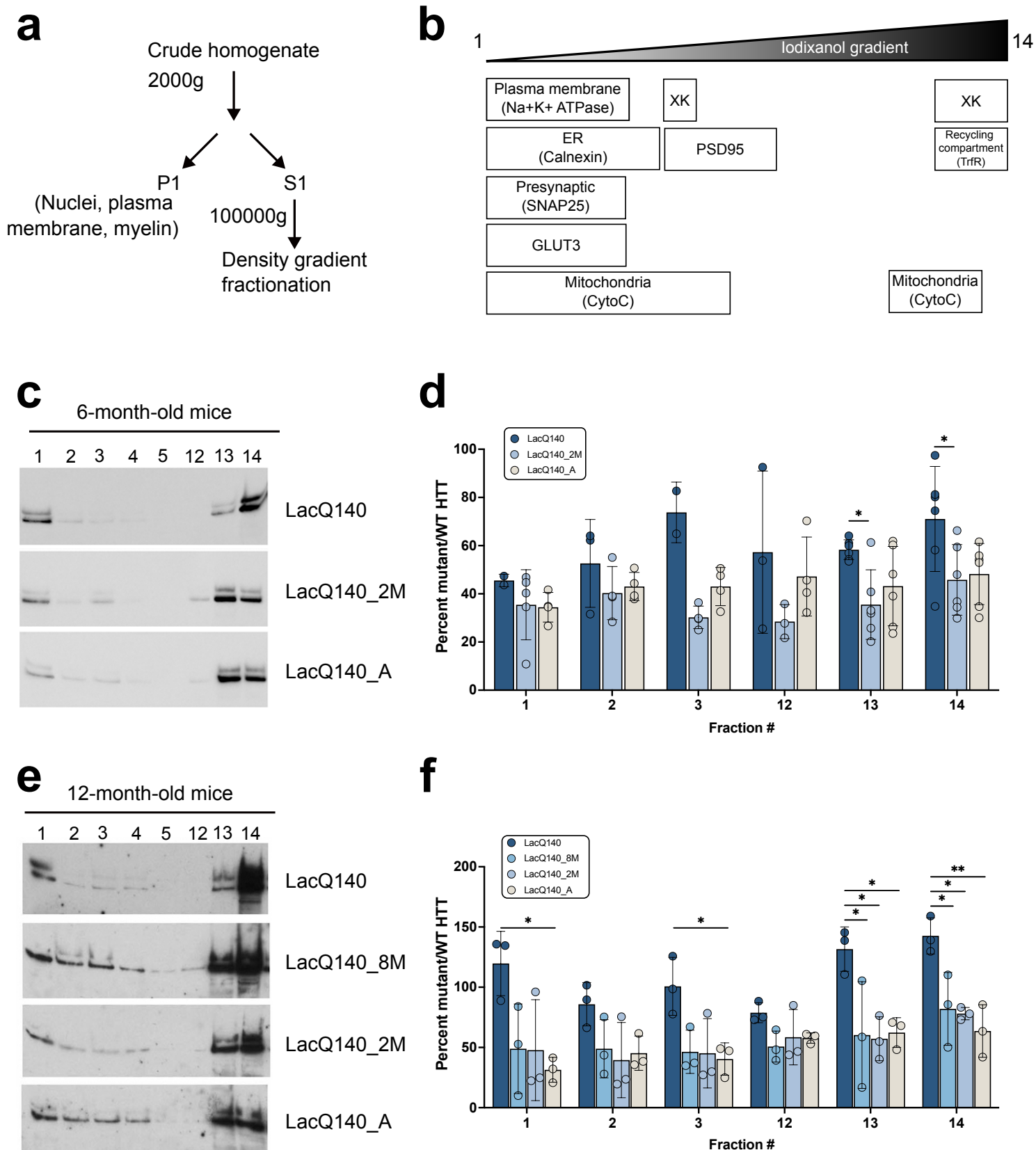
c



Supplementary Figure 1. Analysis of mHTT protein levels with EPR5526 and PHP3 in crude homogenates of 6-, 9- and 12-months old mice.

HTT levels were analyzed by western blot on equal amounts of protein (10 μ g) using anti-HTT antibody EPR5526 and anti-polyQ antibody PHP3. Total pixel intensity quantification for each band measured using ImageJ software in 6-month-old mice shows a significant decrease in WT HTT as detected with EPR5526 in all LacQ140 mice compared to WT mice but no change in mHTT levels (**a**). mHTT levels are significantly lower in LacQ140_2M and LacQ140_A mice as detected with PHP3 compared to LacQ140 (**a**, -42% and -35% respectively, ** $p < 0.01$, *** $p < 0.001$, One-way ANOVA with Tukey's multiple comparison test, $n=6$). Total pixel intensity quantification in 9-month-old mice shows a significant decrease in WT HTT as detected with EPR5526 in all LacQ140 mice compared to WT mice. (**b**). mHTT levels are significantly lower in LacQ140_2M and LacQ140_A mice as detected with EPR5526 and PHP3 compared to LacQ140 (**b**, EPR5526: -24% and -30%, respectively; PHP3: -46% and -49% respectively, * $p < 0.05$, ** $p < 0.01$, *** $p < 0.001$, One-way ANOVA with Tukey's multiple comparison test, $n=6$). Total pixel intensity quantification in 12-month-old mice shows a significant decrease in WT HTT as detected with EPR5526 in LacQ140 and LacQ140_2M compared to WT mice. No changes in mHTT levels as detected with either EPR5526 or PHP3 were observed (**c**).

Supplementary Figure 2

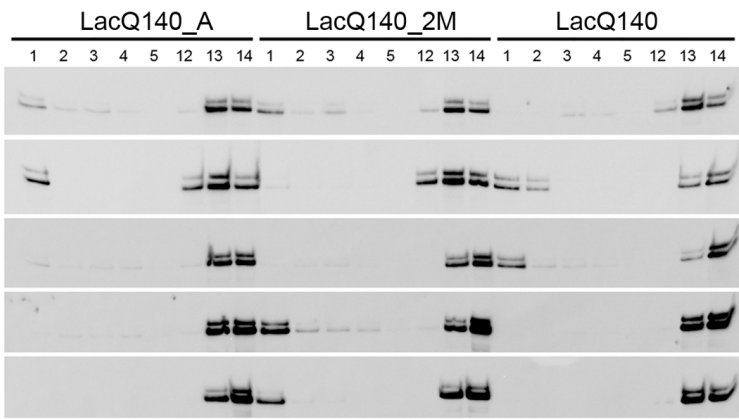


Supplementary Figure 2. Effects of mHtt lowering on the subcellular distribution of WT and mHTT protein by density gradient ultracentrifugation.

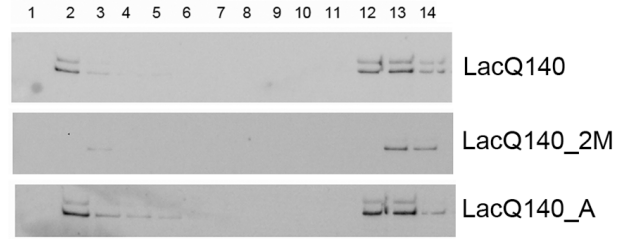
Diagram depicts the centrifugation strategy for protein samples **(a)**. Schematic shows the approximate location in the fractions of protein markers and the organelles found in these compartments **(b)**. Representative western blot images for equal volumes of fractions 1-5 and 12-14 from 6-month-old mice probed with anti-HTT antibody Ab1 are shown in **(c)**. The remaining images are shown in **Supplementary Figure 3a**. Total pixel intensity quantification for each band measured using ImageJ software is graphed as average percent mutant/WT HTT \pm SD for each fraction **(d)**. Since each fraction contains different levels of proteins normally used to control for protein loading, levels of mHTT were normalized to levels of WT HTT which was not repressed/lowered. The ratio mutant/WT HTT is significantly higher in LacQ140 mice compared to LacQ140_2M in fractions 13 and 14 (* $p < 0.05$, One-way ANOVA with Tukey's multiple comparison test for each fraction, $n=6$). Representative western blot images for equal volumes of fractions 1-4 and 11-14 from 12-month-old mice probed with anti-HTT antibody Ab1 are shown in **(e)**. The remaining images are shown in **Supplementary Figure 3c**. Total pixel intensity quantification for each band is graphed as average percent mutant/WT HTT \pm SD for each fraction **(f)**. The ratio mutant/WT HTT is significantly higher in LacQ140 compared to LacQ140_8M, LacQ140_2M and/or LacQ140_A mice in fractions 1, 3, 13, and 14 (* $p < 0.05$, ** $p < 0.01$, One-way ANOVA with Tukey's multiple comparison test for each fraction, $n=3$). Graphs indicate data in fractions where mHTT was detected in at least 3 mice except LacQ140_A fractions 1 and 3 where only 2 mice had detectible mHTT.

Supplementary Figure 3

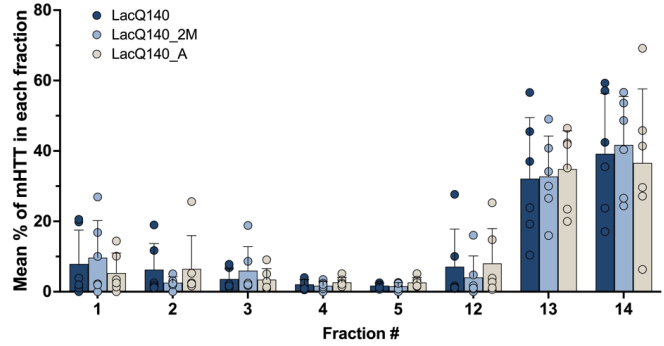
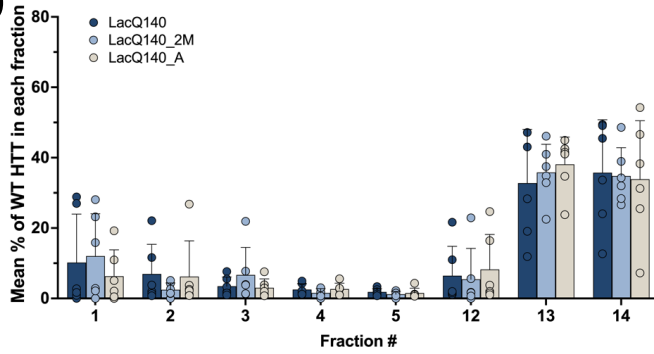
a



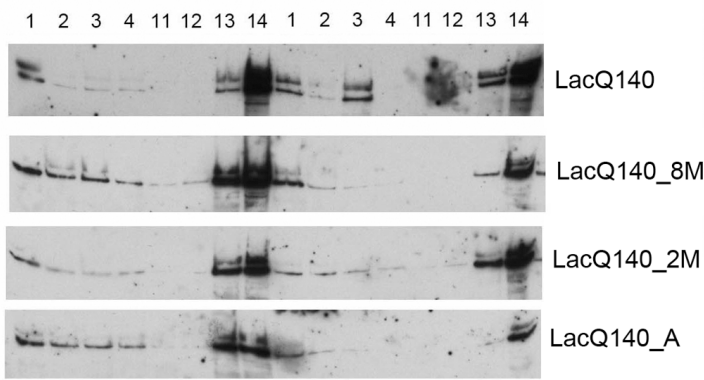
6 month old mice



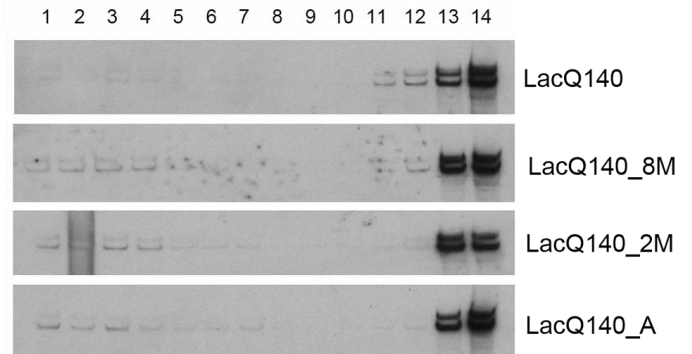
b



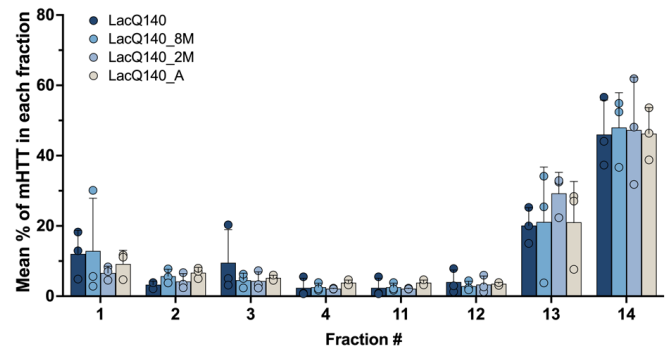
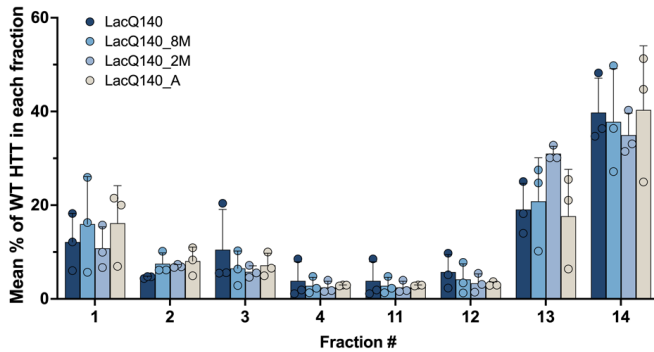
c



12 month old males



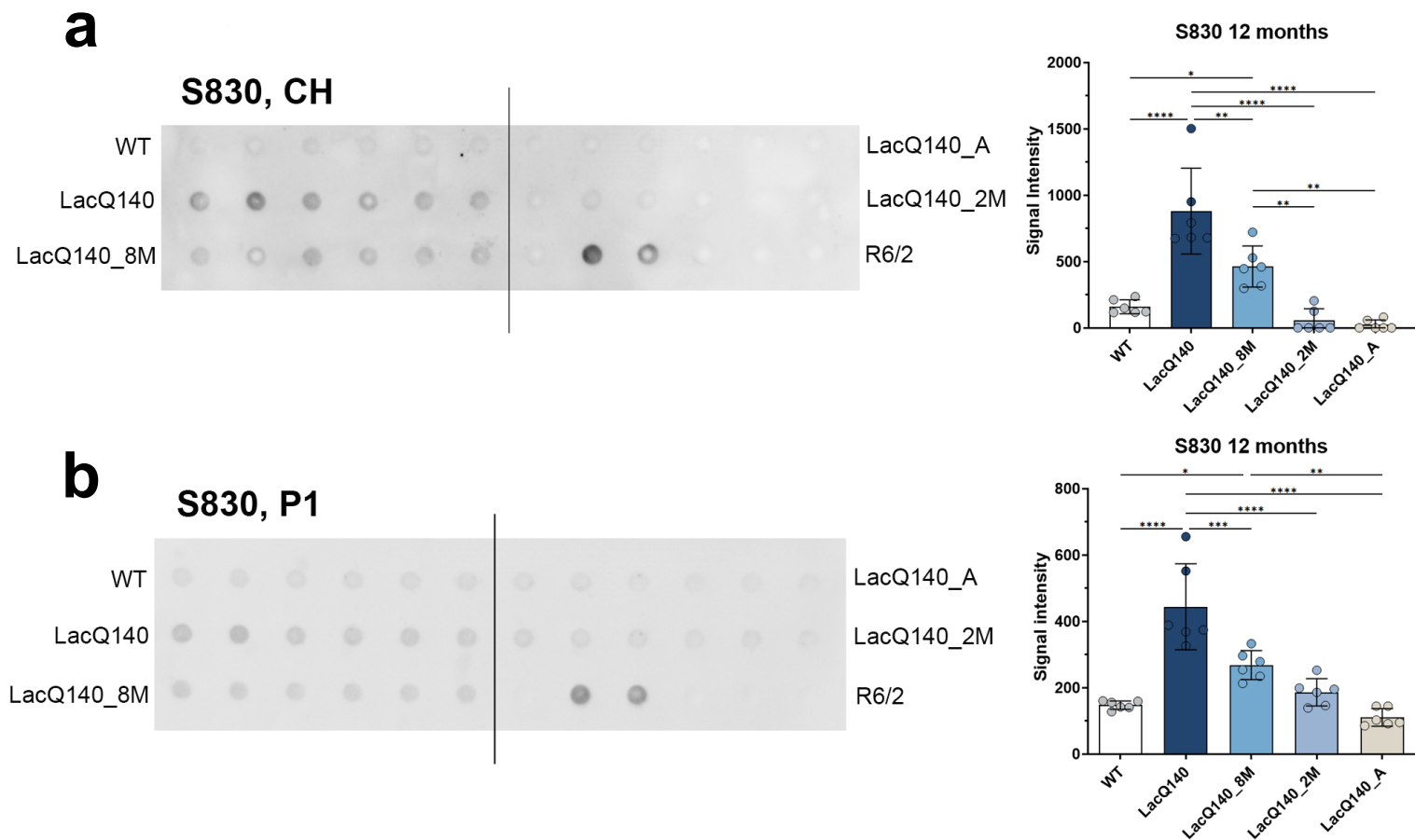
d



Supplementary Figure 3. Effects of mHtt lowering on the subcellular distribution of WT and mHTT.

Western blot images for equal volumes of fractions 1-14 (right blots, each strip is from one mouse) or fractions 1-5 and 12-14 (left blots) from 6-month-old mice probed with anti-HTT antibody Ab1 are shown in **(a)**. Each strip in left blots is a set of 1 mouse per treatment group with the groups labeled at the top of the blots. Total pixel intensity quantification for each band using ImageJ software is graphed as average percent of total HTT signal for each fraction \pm SD **(b)**. Representative western blot images for equal volumes of fractions 1-14 (right blots, each strip is from one mouse) or 1-4 and 11-14 (left blots) from 12-month-old mice probed with anti-HTT antibody Ab1 are shown in **(c)**. Each strip in the left blots is from 2 mice per group with the groups labeled on the right. Total pixel intensity quantified for each band using ImageJ software are graphed as average percent of total HTT signal for each fraction \pm SD **(d)**. There is no difference in WT or mHTT levels as a percent of total HTT in any fraction with any treatment of LacQ140 mice at 6 or 12 months (One-way ANOVA with Tukey's multiple comparison test for each fraction, n=6 for 6 months and n=3 for 12 months).

Supplementary Figure 4



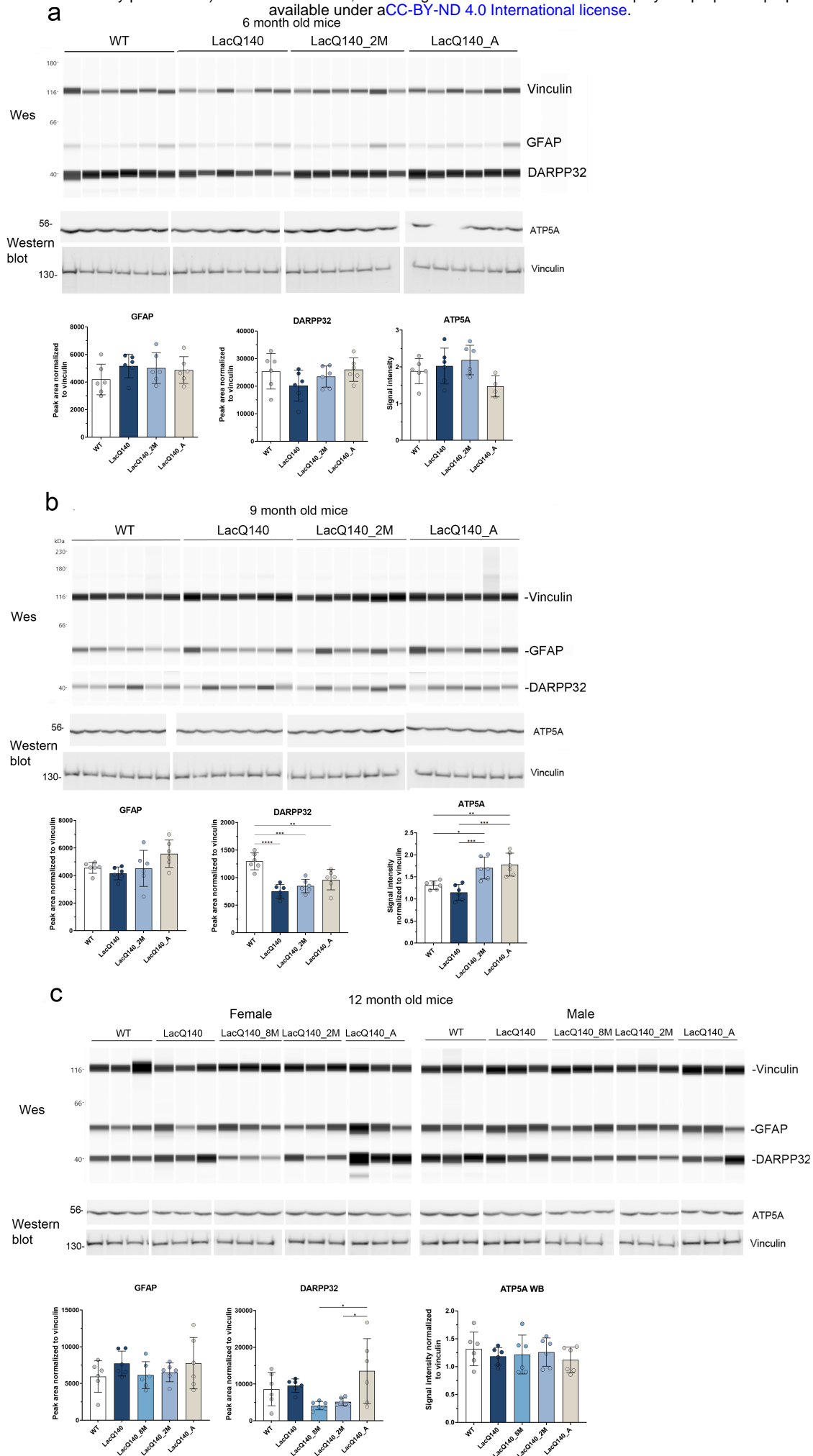
Supplementary Figure 4. HTT levels in crude homogenates and P1 fractions from WT and LacQ140 mice by filter trap assay.

Filter trap assays of 12-month-old crude homogenates **(a)** and P1 fractions **(b)** were probed with S830 antibody. Each dot represents one animal and each of the 6 dots across equals one group which is labeled on the left and right sides. There are 2 dots for the lysates from R6/2 HD mice which have a highly expressing transgene for a small fragment of HTT containing a large CAG repeat (180CAGs) and that accumulate numerous aggregates which have been shown to be retained in the assay and were used as a positive control. There was significantly more signal for aggregated mHTT in the 12-month-old LacQ140 mice compared to WT, LacQ140_8M, LacQ140_2M and LacQ140_A mice **(a)**, * $p < 0.05$, ** $p < 0.01$, **** $p < 0.0001$, One-way ANOVA with Tukey's multiple comparison test, $n=6$). In the P1 fractions, there was significantly more signal for aggregated mHTT detected with S830 antibody in the 12-month LacQ140 mice compared to WT, LacQ140_8M, LacQ140_2M and LacQ140_A mice and in LacQ140_8M compared to WT and LacQ140_A mice **(b)**, * $p < 0.05$, ** $p < 0.01$, *** $p < 0.001$, **** $p < 0.0001$, One-way ANOVA with Tukey's multiple comparison test, $n=6$).

Supplementary Figure 5. Duration of *mHtt* lowering in 6, 9 and 12 months old LacQ140 mice affects levels of PDE10A and SCN4B.

PDE10A and SCN4B levels were analyzed by western blot on equal amounts of protein (10 μ g). Total pixel intensity quantification for each band using ImageJ software in 6-month-old mice shows a significant decrease in PDE10A levels in LacQ140 compared to WT mice. There is an increase in PDE10A levels in LacQ140_2M and LacQ140_A mice compared to LacQ140 and no change from WT mice (**a**, * $p < 0.05$, ** $p < 0.01$, **** $p < 0.0001$, One-way ANOVA with Tukey's multiple comparison test, $n=6$). There is a significant decrease in SCN4B levels in LacQ140 compared to WT mice and a significant increase back to WT levels in LacQ140_2M mice. Total pixel intensity quantification in 9-month-old mice shows a significant decrease in PDE10A levels in LacQ140 compared to WT mice. There is an increase in PDE10A levels in LacQ140_2M compared to LacQ140 and no change from WT mice (**b**, ** $p < 0.01$, *** $p < 0.001$, One-way ANOVA with Tukey's multiple comparison test, $n=6$). There is a significant decrease in SCN4B levels in LacQ140 compared to WT mice. There is a significant increase in SCN4B levels in LacQ140_2M and LacQ140_A mice compared to LacQ140 but significantly lower than in the WT mice (**b**, * $p < 0.05$, ** $p < 0.01$, *** $p < 0.001$, **** $p < 0.0001$, One-way ANOVA with Tukey's multiple comparison test, $n=6$). Total pixel intensity quantification in 12-month-old mice shows a significant decrease in PDE10A levels in LacQ140, LacQ140_8M and LacQ140_2M compared to WT mice. There is an increase in PDE10A levels in LacQ140_A mice compared to LacQ140 and LacQ140_2M and no change from WT mice (**c**, * $p < 0.05$, ** $p < 0.01$, *** $p < 0.001$, One-way ANOVA with Tukey's multiple comparison test, $n=6$). There are no changes in SCN4B levels in any of the LacQ140 or WT mice.

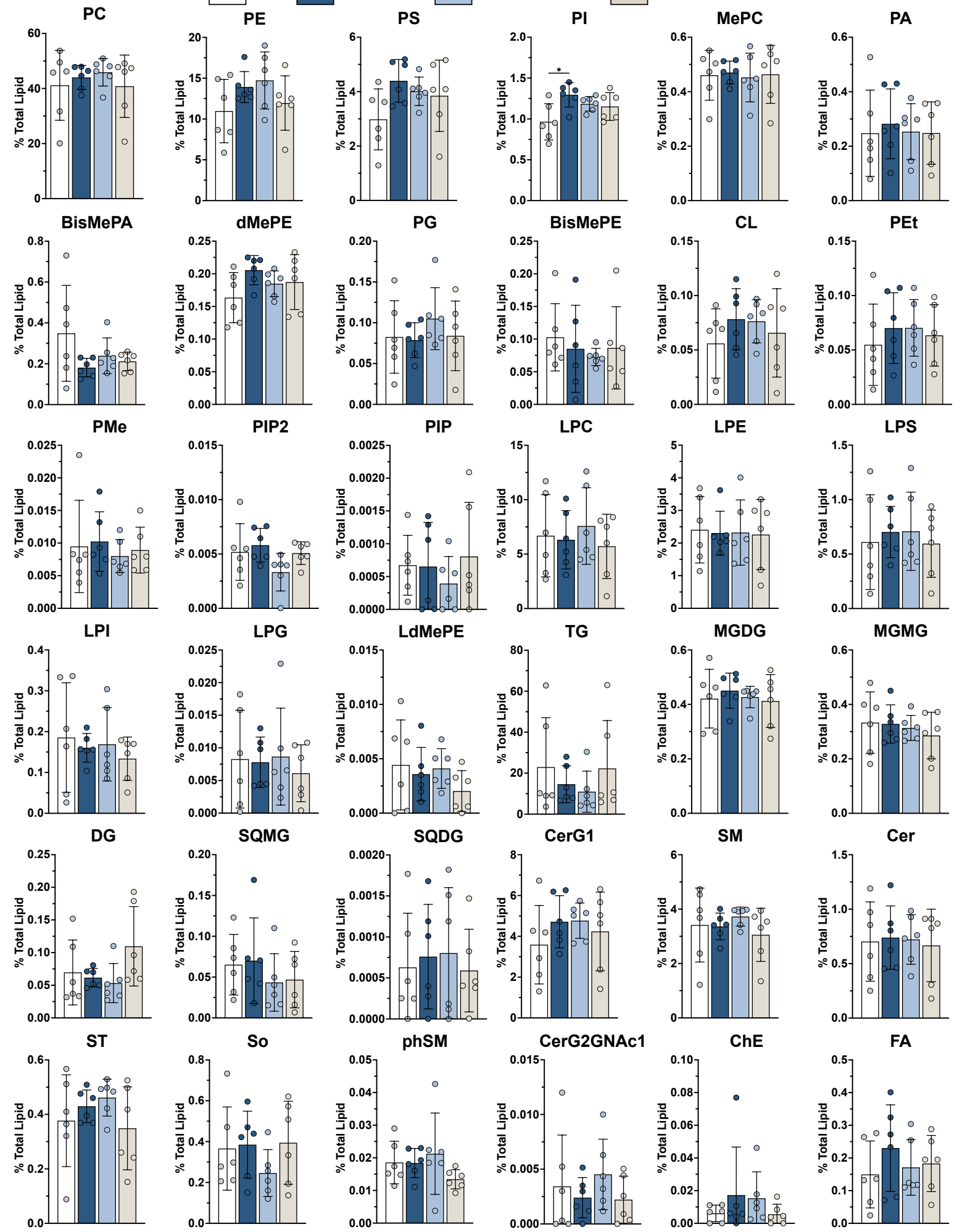
Supplementary Figure 6



Supplementary Figure 6. Duration of *mHtt* lowering in 6, 9 and 12 months old LacQ140 mice has minimal effects on levels of GFAP, DARPP32 and ATP5A.

GFAP and DARPP32 levels were analyzed by capillary immunoassay on equal amounts of protein (0.6 µg) and ATP5A levels were analyzed by western blot on equal amounts of protein (10 µg). In 6-month-old mice, peak area analysis shows no significant change in GFAP or DARPP32 levels (**a**) and total pixel intensity quantification shows no changes in ATP5A levels in any of the LacQ140 or WT mice (**a**). Peak area analysis in 9-month-old mice shows a significant decrease in DARPP32 levels in all LacQ140 mice compared to WT mice (**b**, ** $p < 0.01$, *** $p < 0.001$, One-way ANOVA with Tukey's multiple comparison test, $n=6$). Total pixel intensity quantification shows ATP5A levels are significantly higher in LacQ140_2M and LacQ140_A mice compared to WT or LacQ140 mice (**b**, * $p < 0.05$, ** $p < 0.01$, *** $p < 0.001$, One-way ANOVA with Tukey's multiple comparison test, $n=6$). Peak area analysis in 12-month-old mice shows no significant change in GFAP levels in LacQ140 or WT mice. There is a significant decrease in DARPP32 levels in LacQ140_8M and LacQ140_2M compared to LacQ140_A mice (**c**, * $p < 0.05$, One-way ANOVA with Tukey's multiple comparison test, $n=6$). Total pixel intensity quantification for each band using ImageJ software shows no changes in ATP5A levels in any of the LacQ140 or WT mice.

WT LacQ140 LacQ140_2M LacQ140_A



Supplementary Figure 7. Lipid subclasses detected in caudate putamen of 6-month-old mice.

Lipids were extracted and analyzed by LC-MS/MS. Graphs show relative intensities for indicated lipid subclasses expressed as a percent of total lipid intensity per sample for each genotype or treatment group. Plotted values represent summed lipid subclass intensity standardized to total amount of lipid detected in the same sample. Bar charts underneath individual points represent group means and error bars are \pm standard deviation. PI was significantly increased in striatum of 6-month-old LacQ140 mice compared to WT mice (One-way ANOVA with Tukey's multiple comparisons test, $F(3, 20) = 4.176$, * $P=0.0189$, $n=6$). This increase is not significant when p-values are adjusted for multiple testing using the Benjamini, Krieger and Yekutieli procedure with a false discovery rate of 5%, ($q = 0.7144$, $N=36$ subclasses). No changes between groups were found in any other subclasses.

Abbreviations:

Glycerophospholipids: PC = phosphatidylcholine, PE = phosphatidylethanolamine, PS = phosphatidylserine, PI = phosphatidylinositol, MePC = methylphosphocholine, PA = phosphatidic acid, BisMePA = bis-methyl phosphatidic acid, dMePE = dimethyl phosphatidylethanolamine, PG = phosphatidylglycerol, BisMePE = bis-methyl phosphatidylethanolamine, CL = cardiolipin, PEt = phosphatidylethanol, PMe = phosphatidylmethanol, PIP2 = phosphatidylinositol-bisphosphate, PIP = phosphatidylinositol-monophosphate, LPC = lysophosphatidylcholine, LPE = lysophosphatidylethanolamine, LPS = lysophosphatidylserine, LPI = lysophosphatidylinositol LPG = lysophosphosphatidylglycerol, LdMePE = lysodimethyl phosphatidyl ethanolamine

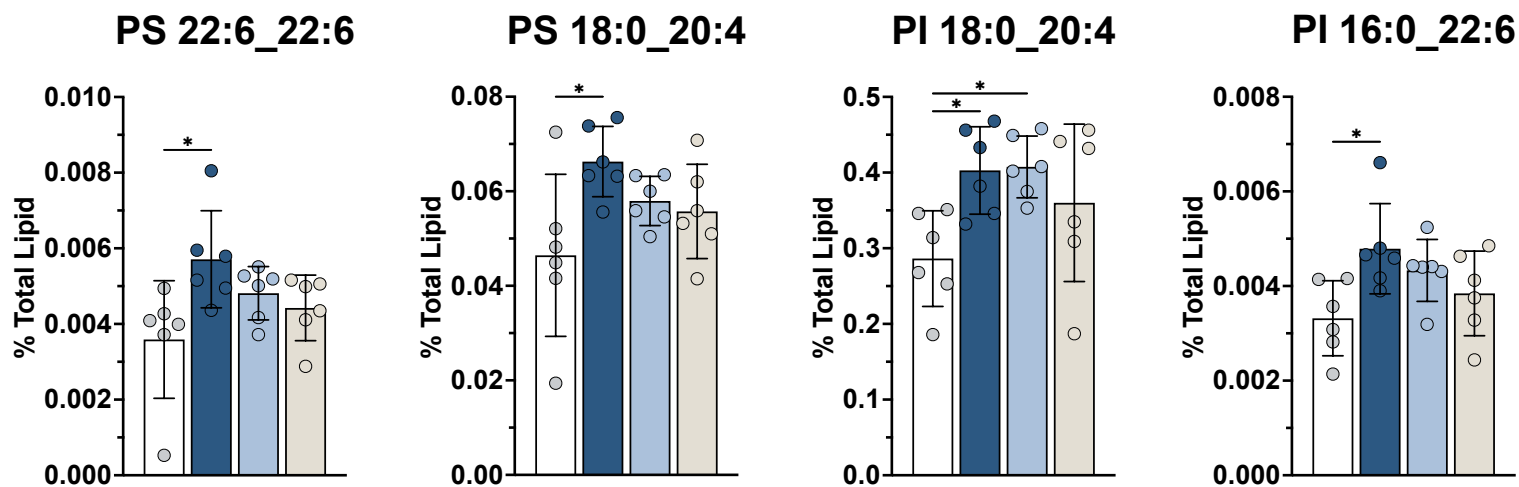
Glycerolipids: TG = triacylglycerol, MGDG = monogalactosyldiacylglycerol, MGMG = monogalactosylmonoacylglycerol, DG = diacylglycerol, SQMG = sulfoquinovosylmonoacylglycerol, SQDG = sulfoquinovosyldiacylglycerol,

Sphingolipids: CerG1 = simple Glc series, SM = sphingomyelin, Cer = ceramide, ST = sulfatide, So = sphingosine, phSM = sphingomyelin phytosphingosine, CerG2GNac1 = Simple Glc series

Sterol lipids: ChE = cholesterol ester

Fatty acyls: FA = fatty acid

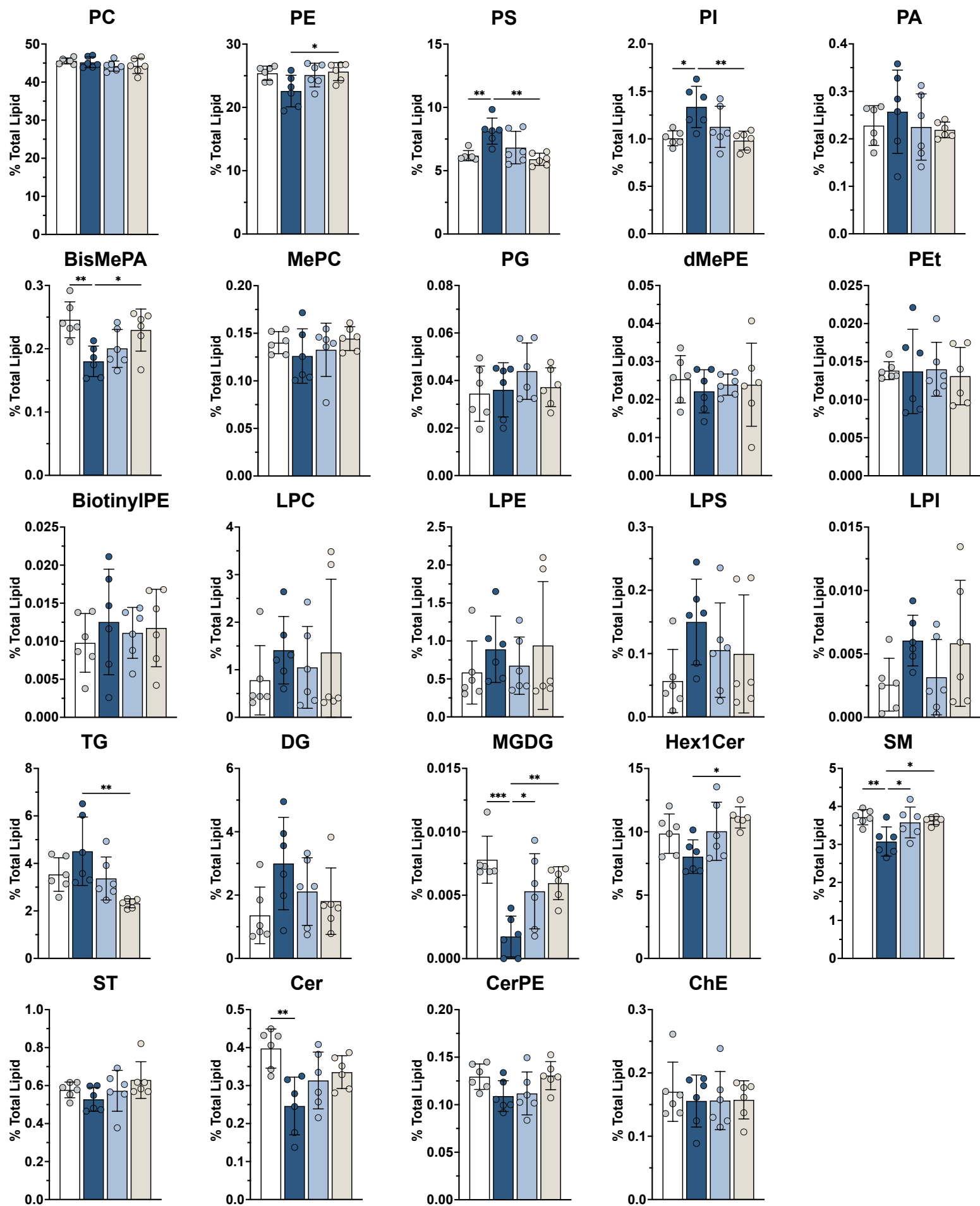
WT LacQ140 LacQ140_2M LacQ140_A



Supplementary Figure 8. Individual lipid species significantly different between 6-month-old LacQ140 and WT mice.

Lipids were extracted and analyzed by LC-MS/MS. Graphs show relative intensities for indicated lipid species expressed as a percent of total lipid intensity per sample for each genotype or treatment group. Plotted values represent individual lipid species intensity standardized to total amount of lipid detected in the same sample. Bar charts underneath individual points represent group means and error bars are \pm standard deviation. One-way analysis of variance (ANOVA) was used to evaluate differences in lipid species intensity between groups and Tukey's multiple comparisons test was used for post-hoc pairwise comparisons (n=6 mice per group, * $p < 0.05$, Tukey's multiple comparisons test). To correct for multiple testing over all lipids analyzed, the Benjamini, Krieger and Yekutieli procedure was used with a false discovery rate of 5% (N=800 lipid species), FDR adjusted p-values are reported as q values. No individual species found to be different by one-way ANOVA were significant following correction of p-values. PS 22:6_22:6: $F(3, 20) = 3.812$, * $P=0.0260$, $q=1$, ns; PS 18:0_20:4: $F(3, 20) = 3.349$, * $P=0.0396$, $q=1$, ns; PI 18:0_20:4: $F(3, 20) = 3.812$, * $P=0.0260$, $q=1$, ns; PI 16:0_22:6: $F(3, 20) = 3.466$, * $P=0.0356$, $q=1$, ns. Abbreviations: PI = phosphatidylinositol, PS = phosphatidylserine

WT LacQ140 LacQ140_2M LacQ140_A



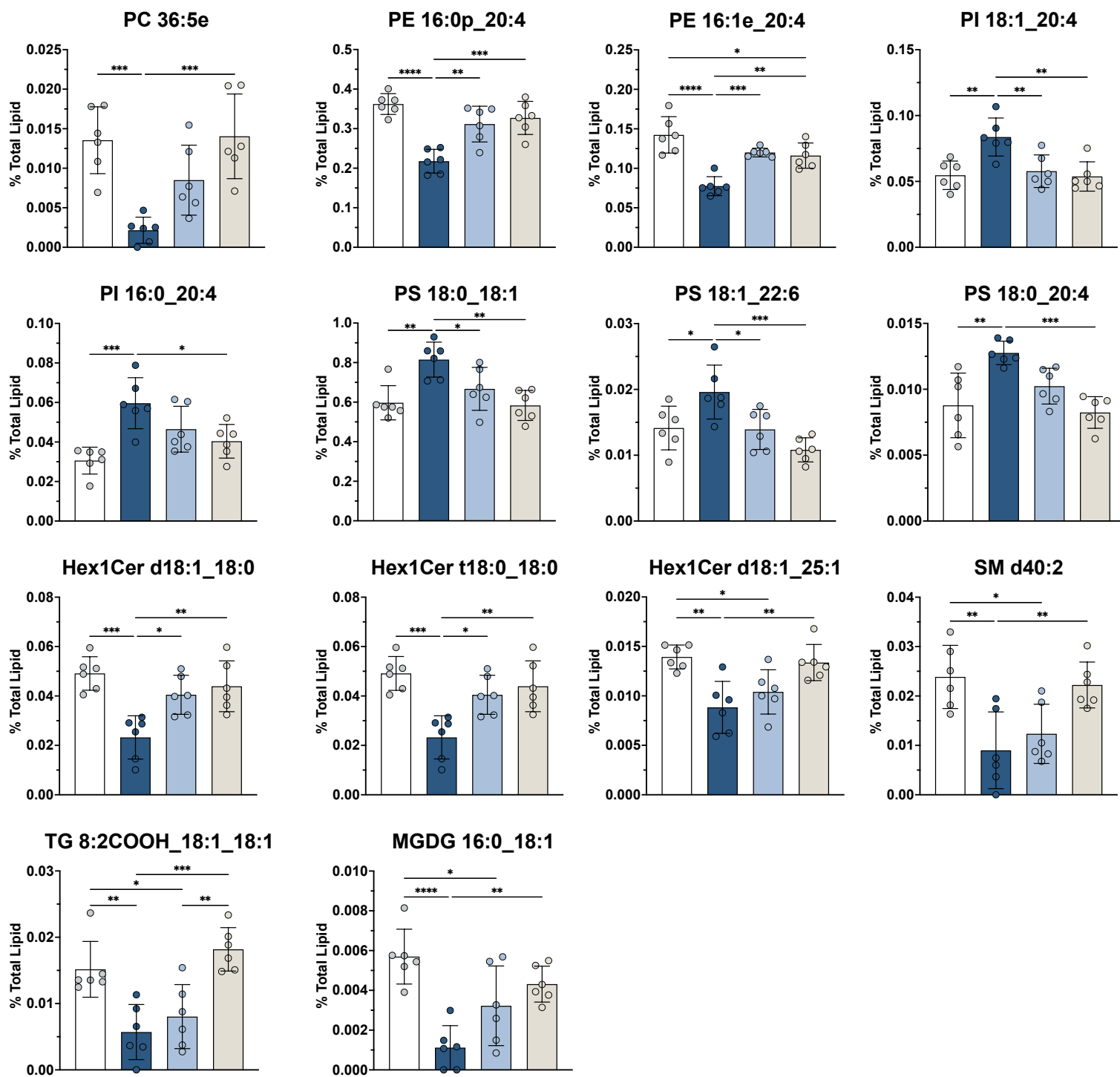
Supplementary Figure 9. Lipid subclasses detected in caudate putamen of 9-month-old mice.

Lipids were extracted and analyzed by LC-MS/MS. Graphs show relative intensities for indicated lipid subclasses expressed as a percent of total lipid intensity per sample for each genotype or treatment group. Plotted values represent summed lipid subclass intensity standardized to total amount of lipid detected in the same sample. Bar charts underneath individual points represent group means and error bars are \pm standard deviation. One-way analysis of variance (ANOVA) was used to evaluate differences in lipid subclass intensity between groups and Tukey's multiple comparisons test was used for post-hoc pairwise comparisons ($n=6$ mice per group, $*p < 0.05$, $**p < 0.01$, Tukey's multiple comparisons test). To correct for multiple testing the Benjamini, Krieger and Yekutieli procedure was used with a false discovery rate of 5% ($N=24$ subclasses) and FDR adjusted p-values are reported as q values. PS: $F(3, 20) = 7.601$, $**P=0.0014$, $q=0.0125$, PI: $F(3, 20) = 5.707$, $**P=0.0054$, $q=0.0168$, BisMePA: $F(3, 20) = 6.086$, $**P=0.0041$, $q=0.0168$, SM: $F(3, 20) = 5.465$, $**P=0.0066$, $q=0.0168$, Cer: $F(3, 20) = 5.883$, $**P=0.0048$, $q=0.0168$, MGDG: $F(3, 20) = 9.350$, $***P=0.0005$, $q=0.0089$. PE, TG and Hex1Cer were unchanged between LacQ140 and WT groups but had changes among other treatment groups (PE: $F(3, 20) = 3.717$, $*P=0.0284$, $q=0.0563$, ns, TG: $F(3, 20) = 5.637$, $**P=0.0057$, $q=0.0168$, Hex1Cer: $F(3, 20) = 3.891$, $*P=0.0243$, $q=0.054$, ns).

Abbreviations:

Glycerophospholipids: PC = phosphatidylcholine, PE = phosphatidylethanolamine, PS = phosphatidylserine, PI = phosphatidylinositol, PA = phosphatidic acid, BisMePA = bis-methyl phosphatidic acid, MePC = methylphosphocholine, PG = phosphatidylglycerol, dMePE = dimethyl phosphatidylethanolamine, PEt = phosphatidylethanol, BiotinylPE = biotinyl-phosphoethanolamine, LPC = lysophosphatidylcholine, LPE = lysophosphatidylethanolamine, LPS = lysophosphatidylserine, LPI = lysophosphatidylinositol
Glycerolipids: TG = triacylglycerol, DG = diacylglycerol, MGDG = monogalactosyldiacylglycerol
Sphingolipids: Hex1Cer = monohexosylceramide, SM = sphingomyelin, ST = sulfatide, Cer = ceramide, CerPE = ceramide phosphorylethanolamine
Sterol lipids: ChE = cholesterol ester

WT LacQ140 LacQ140_2M LacQ140_A



Supplementary Figure 10. Individual lipid species significantly changed between 9-month-old LacQ140 and WT mice.

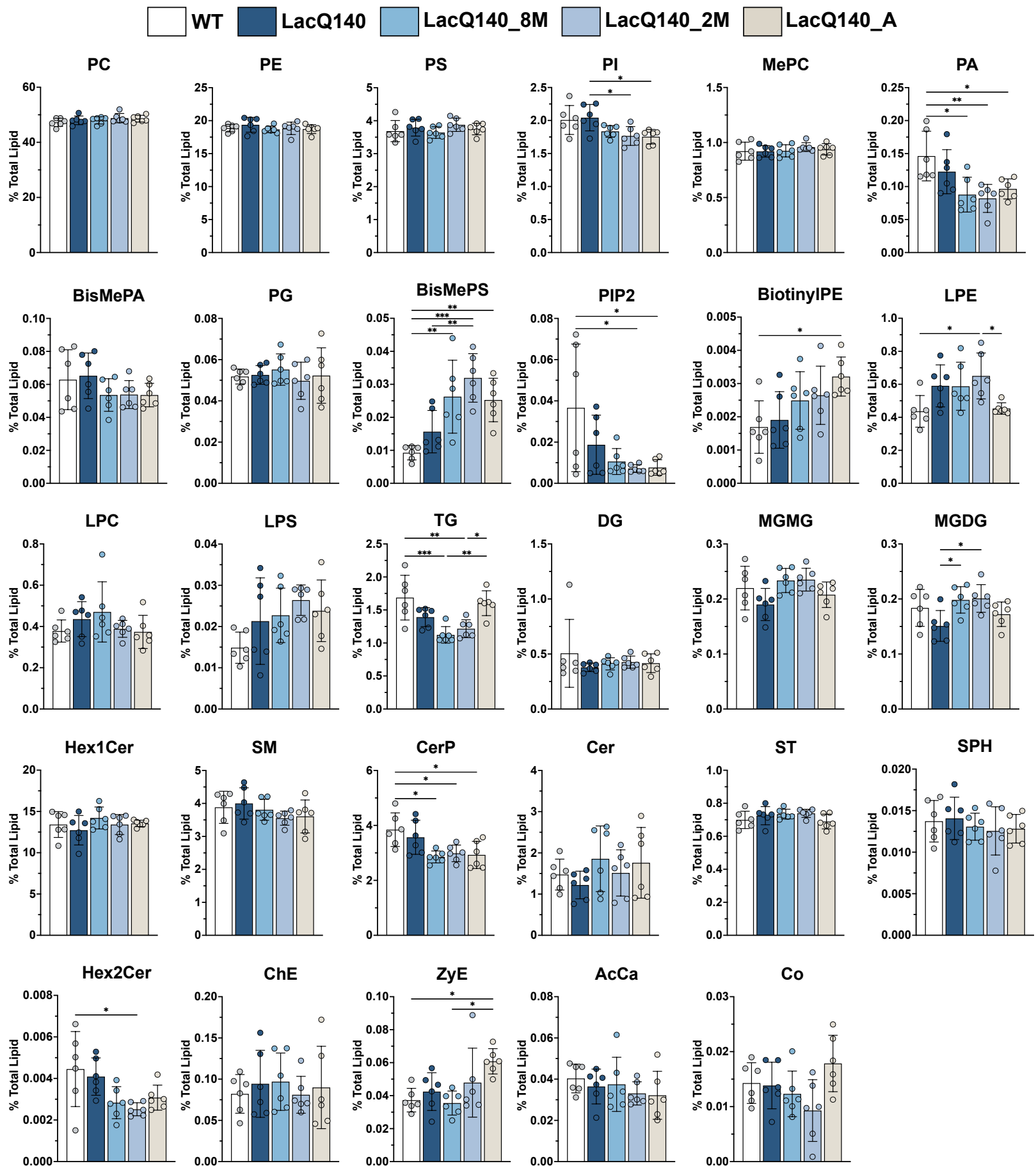
Lipids were extracted and analyzed by LC-MS/MS. Graphs show relative intensities for indicated lipid species expressed as a percent of total lipid intensity per sample for each genotype or treatment group. Plotted values represent individual lipid species intensity standardized to total amount of lipid detected in the same sample. Bar charts underneath individual points represent group means and error bars are \pm standard deviation. One-way analysis of variance (ANOVA) was used to evaluate differences in lipid species intensity between groups and Tukey's multiple comparisons test was used for post-hoc pairwise comparisons (n=6 mice per group, *p < 0.05, **p < 0.01, ***p < 0.001, ****p < 0.0001, Tukey's multiple comparisons test). To correct for multiple testing over all lipids analyzed, the Benjamini, Krieger and Yekutieli procedure was used with a false discovery rate of 5% (N=632 lipid species), FDR adjusted p-values are reported as q values. PC 36:5e: F(3, 20) = 10.68, ***P=0.0002, q=0.02, PE 16:1e_20:4: F(3, 20) = 18.14, ****P<0.0001, q=0.003, PE 16:0p_20:4: F(3, 20) = 16.97, ****P<0.0001, q=0.003, PI 18:1_20:4: F(3, 20) = 8.086, **P=0.0010, q=0.041, PI 16:0_20:4: F(3, 20) = 8.449, ***P=0.0008, q=0.039, PS 18:0_18:1: F(3, 20) = 8.226, ***P=0.0009, q=0.041, PS 18:1_22:6: F(3, 20) = 7.916, **P=0.0011, q=0.042, PS 18:0_20:4: F(3, 20) = 9.739, ***P=0.0004, q=0.023, Hex1Cer d18:1_18:0: F(3, 20) = 10.37, ***P=0.0002, q=0.02, Hex1Cer t18:0_18:0: F(3, 20) = 10.35, ***P=0.0003, q=0.02, Hex1Cer d18:1_25:1: F(3, 20) = 8.440, ***P=0.0008, q=0.039, SM d40:2: F(3, 20) = 8.052, **P=0.0010, q=0.041, TG 8:2COOH_18:1_18:1: F(3, 20) = 11.98, ***P=0.0001, q=0.017, MGDG 16:0_18:1: F(3, 20) = 11.28, ***P=0.0002, q=0.019.

Abbreviations:

Glycerophospholipids: PC = phosphatidylcholine, PE = phosphatidylethanolamine, PI = phosphatidylinositol, PS = phosphatidylserine

Sphingolipids: Hex1Cer = monohexosylceramide, SM = sphingomyelin

Glycerolipids: MGDG = monogalactosyldiacylglycerol, TG = triacylglycerol



Supplementary Figure 11. Lipid subclasses detected in caudate putamen of 12-month-old mice.

Lipids were extracted and analyzed by LC-MS/MS. Graphs show relative intensities for indicated lipid subclasses expressed as a percent of total lipid intensity per sample for each genotype or treatment group. Plotted values represent summed lipid subclass intensity standardized to total amount of lipid detected in the same sample. Bar charts underneath individual points represent group means and error bars are \pm standard deviation. One-way analysis of variance (ANOVA) was used to evaluate differences in lipid subclass intensity between groups and Tukey's multiple comparisons test was used for post-hoc pairwise comparisons ($n=6$ mice per group, $*p < 0.05$, $**p < 0.01$, $***p < 0.001$, Tukey's multiple comparisons test). To correct for multiple testing the Benjamini, Krieger and Yekutieli procedure was used with a false discovery rate of 5% ($N=29$ subclasses), FDR adjusted p-values are reported as q values. PI: $F(4, 25) = 4.316$, $**P=0.0086$, $q=0.0338$, PA: $F(4, 25) = 5.537$, $**P=0.0025$, $q=0.0184$, BisMePS: $F(4, 25) = 9.308$, $****P<0.0001$, $q=0.0022$, PIP2: $F(4, 25) = 3.743$, $*P=0.0161$, $q=0.0394$, BiotinylPE: $F(4, 25) = 3.446$, $*P=0.0225$, $q=0.0451$, LPE: $F(4, 25) = 3.957$, $*P=0.0127$, $q=0.035$. TG: $F(4, 25) = 8.593$, $***P=0.0002$, $q=0.0022$, MGMG: $F(4, 25) = 2.765$, $*P=0.0497$, $q=0.0887$, ns, MGDG: $F(4, 25) = 3.491$, $*P=0.0214$, $q=0.0451$. CerP: $F(4, 25) = 5.185$, $**P=0.0035$, $q=0.0193$, Hex2Cer: $F(4, 25) = 4.076$, $*P=0.0112$, $q=0.035$, ZyE: $F(4, 25) = 4.256$, $**P=0.0092$, $q=0.0338$.

Abbreviations:

Glycerophospholipids: PC = phosphatidylcholine, PE = phosphatidylethanolamine, PS = phosphatidylserine, PI = phosphatidylinositol, MePC = methylphosphocholine, PA = phosphatidic acid, BisMePA = bis-methyl phosphatidic acid, PG = phosphatidylglycerol, BisMePS = bis-methylphosphatidylserine, PIP2 = phosphatidylinositol-bisphosphate, BiotinylPE = biotinyl-phosphoethanolamine, LPE = lysophosphatidylethanolamine, LPC = lysophosphatidylcholine, LPS = lysophosphatidylserine

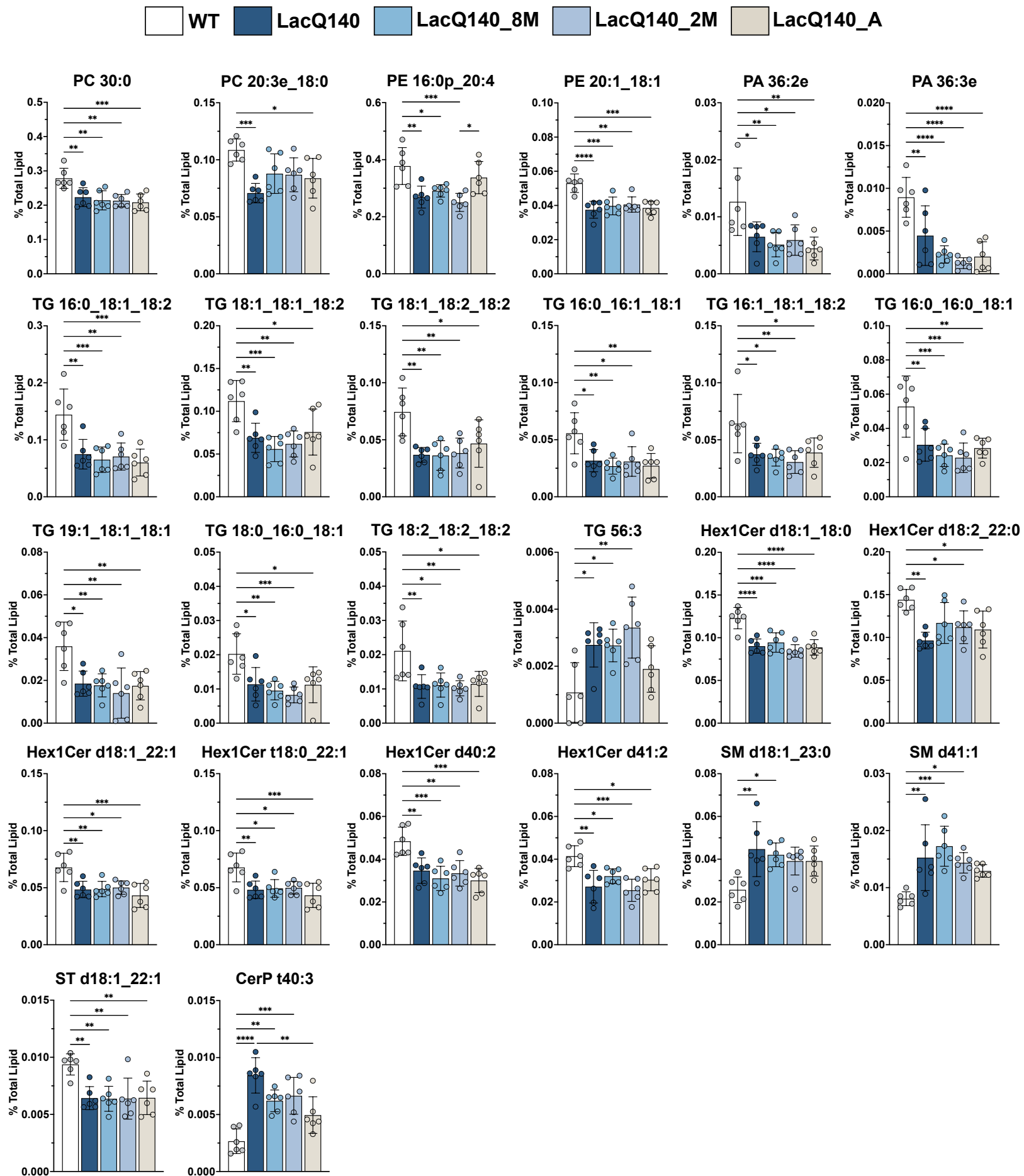
Glycerolipids: TG = triacylglycerol, DG = diacylglycerol, MGMG = monogalactosylmonoacylglycerol, MGDG = monogalactosyldiacylglycerol

Sphingolipids: Hex1Cer = monohexosylceramide, SM = sphingomyelin, CerP = ceramide phosphate, Cer = ceramide, ST = sulfatide, SPH = sphingoid base, Hex2Cer = dihexosylceramide

Sterol lipids: ChE = cholesterol ester, ZyE = zymosterol

Fatty acyls: AcCa = acyl carnitine

Prenol lipids: Co = coenzyme



Supplementary Figure 12. Individual lipid species significantly changed between 12-month-old LacQ140 and WT mice.

Lipids were extracted and analyzed by LC-MS/MS. Graphs show relative intensities for indicated lipid species expressed as a percent of total lipid intensity per sample for each genotype or treatment group. Plotted values represent individual lipid species intensity standardized to total amount of lipid detected in the same sample. Bar charts underneath individual points represent group means and error bars are \pm standard deviation. One-way analysis of variance (ANOVA) was used to evaluate differences in lipid species intensity between groups and Tukey's multiple comparisons test was used for post-hoc pairwise comparisons ($n=6$ mice per group, $*p < 0.05$, $**p < 0.01$, $***p < 0.001$, $****p < 0.0001$, Tukey's multiple comparisons test). To correct for multiple testing over all lipids analyzed, the Benjamini, Krieger and Yekutieli procedure was used with a false discovery rate of 5% ($N=735$ lipid species), FDR adjusted p-values are reported as q values. PC 30:0: $F(4, 25) = 7.601$, $***P=0.0004$, $q=0.0132$, PC 20:3e_18:0: $F(4, 25) = 5.567$, $**P=0.0024$, $q=0.0327$, PE 16:0p_20:4: $F(4, 25) = 7.879$, $***P=0.0003$, $q=0.0114$, PE 20:1_18:1: $F(4, 25) = 10.36$, $****P<0.0001$, $q=0.0038$, PA 36:2e: $F(4, 25) = 5.630$, $**P=0.0023$, $q=0.0327$, PA 36:3e: $F(4, 25) = 13.27$, $****P<0.0001$, $q=0.0007$, TG 16:0_18:1_18:2: $F(4, 25) = 8.357$, $***P=0.0002$, $q=0.0094$, TG 18:1_18:1_18:2: $F(4, 25) = 7.113$, $***P=0.0006$, $q=0.0182$, TG 18:1_18:2_18:2: $F(4, 25) = 6.249$, $**P=0.0013$, $q=0.0272$, TG 16:0_16:1_18:1: $F(4, 25) = 5.794$, $**P=0.0019$, $q=0.0306$, TG 16:1_18:1_18:2: $F(4, 25) = 4.983$, $**P=0.0043$, $q=0.0438$, TG 16:0_16:0_18:1: $F(4, 25) = 7.833$, $***P=0.0003$, $q=0.0114$, TG 19:1_18:1_18:1: $F(4, 25) = 6.060$, $**P=0.0015$, $q=0.0272$, TG 18:0_16:0_18:1: $F(4, 25) = 6.726$, $***P=0.0008$, $q=0.0217$, TG 18:2_18:2_18:2: $F(4, 25) = 5.352$, $**P=0.0030$, $q=0.0345$, TG 56:3: $F(4, 25) = 6.109$, $**P=0.0014$, $q=0.0272$, Hex1Cer d18:1_18:0: $F(4, 25) = 14.49$, $****P<0.0001$, $q=0.0005$, Hex1Cer d18:2_22:0: $F(4, 25) = 5.594$, $**P=0.0023$, $q=0.0327$, Hex1Cer d18:1_22:1: $F(4, 25) = 6.637$, $***P=0.0009$, $q=0.0219$, Hex1Cer t18:0_22:1: $F(4, 25) = 6.181$, $**P=0.0013$, $q=0.0272$, Hex1Cer d40:2: $F(4, 25) = 9.257$, $****P<0.0001$, $q=0.0058$, Hex1Cer d41:2: $F(4, 25) = 7.880$, $***P=0.0003$, $q=0.0114$, SM d18:1_23:0: $F(4, 25) = 5.007$, $**P=0.0042$, $q=0.0438$, SM d41:1: $F(4, 25) = 6.980$, $***P=0.0006$, $q=0.0197$, ST d18:1_22:1: $F(4, 25) = 6.263$, $**P=0.0012$, $q=0.0272$, CerP t40:3: $F(4, 25) = 14.26$, $****P<0.0001$, $q=0.0005$.

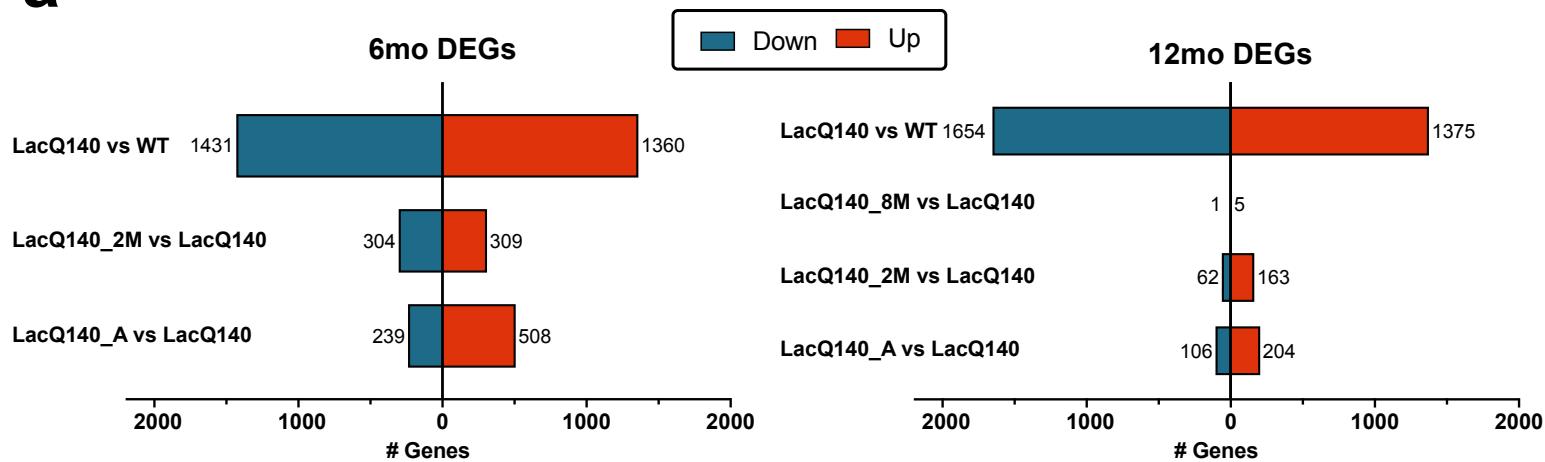
Abbreviations:

Glycerophospholipids: PC = phosphatidylcholine, PE = phosphatidylethanolamine, PA = phosphatidic acid

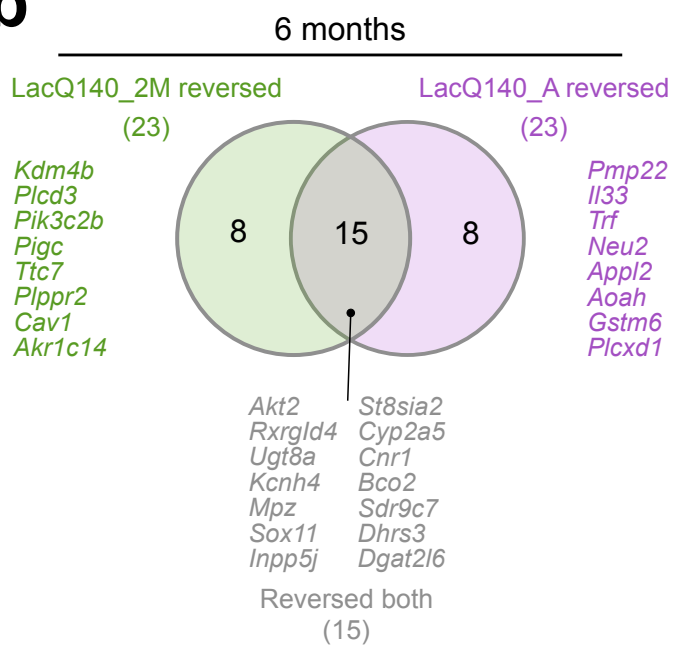
Glycerolipids: TG = triacylglycerol

Sphingolipids: Hex1Cer = monohexosylceramide, SM = sphingomyelin, ST = sulfatide, CerP = ceramide phosphate

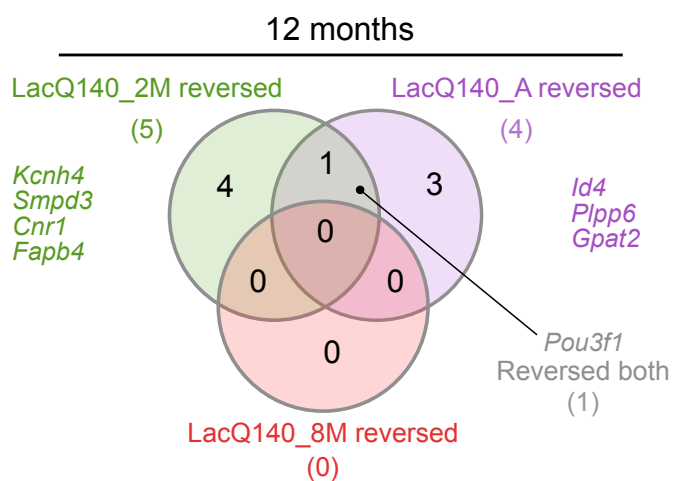
a



b



c



Supplementary Figure 13. DEGs, reversed genes in 6- and 12-month-old LacQ140 mice

(a) Bar chart shows number of differentially expressed genes (DEGs) at 6-months (left) and 12-months (right). Total number of DEGs in LacQ140 mice (upregulated: red and downregulated: blue) are shown in the top bar; lower bars show number of DEGs in mice with mHtt repression (LacQ140_8M, LacQ140_2M, LacQ140_A) compared to LacQ140 mice (i.e., genes “reversed” with mHtt repression). **(b)** Venn diagram depicts genes “reversed” at 6-months for each respective mHtt repression group as shown in **Figure 6c**. **(c)** Venn diagram depicts genes “reversed” at 12-months for each respective mHtt repression group as shown in **Figure 6f**.